

NEAR-INFRARED COLORS OF GAMMA-RAY BURST AFTERGLOWS AND COSMIC REIONIZATION HISTORY

AKIO K. INOUE¹, RYO YAMAZAKI¹, AND TAKASHI NAKAMURA

Department of Physics, Kyoto University, Kyoto 606-8502, Japan

akinoue@tap.scphys.kyoto-u.ac.jp, yamazaki@tap.scphys.kyoto-u.ac.jp, takashi@tap.scphys.kyoto-u.ac.jp

submitted to ApJ

ABSTRACT

Using the near-infrared (NIR) observations of the afterglows of the high redshift ($5 \lesssim z \lesssim 25$) gamma-ray bursts (GRBs) which will be detected by the *Swift* satellite, we discuss a way to study the cosmic reionization history. In principle the details of the cosmic reionization history are well imprinted in the NIR spectra of the GRB afterglows. However the spectroscopy with a space telescope is required to obtain such an information for a very high redshift ($z \gtrsim 15$) unless the neutral fraction of the high- z universe is less than 10^{-6} . The broad-band photometry has the higher sensitivity than that of the spectroscopy, so that the NIR photometric follow-up of the GRB afterglows is very promising to examine the cosmic reionization history. A few minutes exposure with a 8-m class ground-based telescope of the afterglow of the high- z GRBs will reveal how many times the reionization occurred in the universe.

Subject headings: cosmology: observations — gamma rays: bursts — intergalactic medium — radiative transfer — techniques: photometric

1. INTRODUCTION

The evolutionary study of the intergalactic medium (IGM) is now one of the most active fields in astrophysics. Especially, the cosmic reionization history of the IGM attracts many researchers in recent years (see Loeb & Barkana 2001 for a review). Gunn–Peterson trough shortward of the Ly α resonance (Gunn & Peterson 1965) in the spectrum of quasars with redshift $z \sim 6$ indicates that the end of the reionization epoch is $z \sim 6$ (Becker et al. 2001; White et al. 2003). On the other hand, the recent observation of the polarization of the cosmic microwave background (CMB) by *WMAP* suggests that the beginning of the reionization is $z \sim 20$ (Spergel et al. 2003; Kogut et al. 2003). One might think that there is a discrepancy between both observations.

The detailed simulation of the six-dimensional radiative transfer shows that the reionization process proceeds slowly in an inhomogeneous universe (Nakamoto, Umemura, & Susa 2001). If the reionization began at $z \sim 20$, the neutral fraction in the universe decreased gradually, and the universe was ionized almost completely at $z \sim 6$, the apparent discrepancy can be resolved (Wyithe & Loeb 2003a; Haiman & Holder 2003; Ciardi, Ferrara, & White 2003; Chiu, Fan, & Ostricker 2003; Sokasian et al. 2003; Onken & Miralda-Escudé 2003). The scenario that the initial partially ionized epoch was simply followed by the complete ionization can explain the large Thomson scattering opacity observed from the CMB polarization and also is consistent with the previous picture in which the end of the reionization is $z \sim 6$.

Cen (2003a,b) and Wyithe & Loeb (2003b) recently proposed a new scenario of the reionization; the universe was reionized twice. Even in an inhomogeneous universe, enough strong intensity of the ultra-violet (UV) background radiation can ionize the universe quickly. At $z \sim 20$, the first reionization was made by the Population

III (Pop III) stars (metal-free stars) with a top-heavy initial mass function (IMF) which yields a much higher UV emissivity than that of normal Pop I and II stars. Then, the universe was partially recombined at $z \sim 15$ when the transition from the Pop III to II was occurred and the UV emissivity was suddenly suppressed because of the different IMF. Finally, the UV photons from the Pop II stars increased gradually and ionized the universe again at $z \sim 6$.

Cen’s scenario can also resolve the discrepancy, but it is different from others in the history of the cosmic reionization; the first complete ionization was followed by the partially ionized epoch and then the second complete ionization. We should assess whether Cen’s scenario is favored by using other observations. In this paper, an assessment by using the afterglows of the gamma-ray bursts (GRBs) is discussed.

The usefulness of GRBs to investigate the high- z universe is pointed out by many authors (e.g, Lamb & Reichart 2000; Ciardi & Loeb 2000; Barkana & Loeb 2003). It is strongly suggested that the long duration GRBs arise from the collapse of a massive star (Galama et al. 1998; Uemura et al. 2003; Hjorth et al. 2003; Price et al. 2003). Hence, the GRBs can occur at very high- z once the massive stars are formed. For example, the *Swift* satellite² is expected to detect ~ 10 GRBs per year occurring at $z \gtrsim 10$ (Lamb & Reichart 2000). The redshifts of the GRBs can be determined by the Ly α break or Fe lines in the afterglow spectra (Mészáros & Rees 2003). Furthermore, if we fix an observing time from the prompt emission, the observed afterglow flux does not become so faint even for the extremely high- z GRBs because the earlier phase of the afterglow is observed in the cosmological rest frame (Ciardi & Loeb 2000).

In this paper, we show that the near-infrared (NIR) follow-up observations of the GRB afterglows are very use-

¹ Research Fellow of Japan Society for the Promotion of Science.² <http://swift.gsfc.nasa.gov/>

ful to investigate how many times the cosmic reionization occurred. Starting from a brief summary of the IGM opacity by the neutral hydrogen in section 2, we examine the NIR spectra and colors of the GRB afterglows in section 3 and 4, respectively. Then we discuss a way to obtain the cosmic reionization history in section 5.

We adopt a standard set of the Λ CDM cosmology throughout the paper: $H_0 = 70 \text{ km s}^{-1} \text{ Mpc}^{-1}$, $\Omega_M = 0.3$, $\Omega_\Lambda = 0.7$, and $\Omega_b = 0.04$.

2. IGM OPACITY

Suppose an observer at $z = 0$ who observes a source with $z = z_S$ at the observer's frequency ν_0 . The radiation from the source is absorbed by the Lyman series lines and the photoionization of the intervening neutral hydrogen (Gunn & Peterson 1965). The hydrogen cross section at the rest frame frequency ν is

$$\sigma_{\text{HI}}(\nu) = \sigma_{\text{LC}}(\nu) + \sum_i \sigma_i(\nu), \quad (1)$$

where $\sigma_{\text{LC}}(\nu)$ is the cross section for the Lyman continuum photons ($h\nu \geq 13.6 \text{ eV}$) and $\sigma_i(\nu)$ is the cross section for the i -th line of the Lyman series, i.e., $i = \text{Ly}\alpha, \text{Ly}\beta, \text{Ly}\gamma$, etc. Here we consider the lines up to $i = 40$. The optical depth for the observer's frequency ν_0 is given by

$$\tau_{\nu_0}(z_S) = \tau_{\nu_0}^{\text{LC}}(z_S) + \sum_i \tau_{\nu_0}^i(z_S), \quad (2)$$

$$\tau_{\nu_0}^{\text{LC}}(z_S) = \int_0^{z_S} \sigma_{\text{LC}}(\nu_0[1+z]) n_{\text{HI}}(z) \frac{c dz}{(1+z)H(z)}, \quad (3)$$

and

$$\tau_{\nu_0}^i(z_S) = \int_0^{z_S} \sigma_i(\nu_0[1+z]) n_{\text{HI}}(z) \frac{c dz}{(1+z)H(z)}, \quad (4)$$

where $n_{\text{HI}}(z)$ is the number density of the neutral hydrogen at the redshift z , $H(z)$ is the Hubble constant at the redshift z , and c is the light speed.

The cross section for the Lyman continuum photons is given by $\sigma_{\text{LC}}(\nu) = \sigma_{\text{LC}}(\nu/\nu_L)^{-3}$, where $\sigma_{\text{LC}} = 6.30 \times 10^{-18} \text{ cm}^2$ and the Lyman limit frequency $\nu_L = 3.29 \times 10^{15} \text{ Hz}$ (Osterbrock 1989). Thus, we obtain

$$\tau_{\nu_0}^{\text{LC}}(z_S) = \sigma_{\text{LC}} \left(\frac{\nu_L}{\nu_0} \right)^3 n_{\text{H},0} c \int_{z_{\text{min}}}^{z_S} \frac{x_{\text{HI}}(z) dz}{(1+z)H(z)}, \quad (5)$$

where $x_{\text{HI}}(z)$ is the neutral fraction at the redshift z and $z_{\text{min}} = \max[0, (\nu_L/\nu_0) - 1]$. The neutral fraction $x_{\text{HI}}(z)$ is defined as $n_{\text{HI}}(z)/n_{\text{H}}(z)$, where $n_{\text{H}}(z) = n_{\text{H},0}(1+z)^3$ is the cosmic mean number density of hydrogen atom at the redshift z with $n_{\text{H},0}$ being the present one. The effect of the inhomogeneity of the universe can be expressed in the definition of x_{HI} (see below). Since we need the condition $z_{\text{min}} < z_S$ to integrate Eq. (5), $\tau_{\nu_0}^{\text{LC}}(z_S) = 0$ when $\nu_0 \leq \nu_L/(1+z_S)$.

Although the neutral fraction, $x_{\text{HI}}(z)$, might be different for each line of sight, an averaged one is determined by the UV intensity of the background radiation and the inhomogeneity of the hydrogen number density at the redshift z . If the ionization equilibrium is assumed³, the mean neutral fraction is given by $x_{\text{HI}} = C n_e \alpha / \Gamma_{\text{HI}}$, where $C = \langle \rho_{\text{H}}^2 \rangle / \langle \rho_{\text{H}} \rangle^2$ is the clumping factor, n_e is the electron number density, α is the recombination coefficient, and

$\Gamma_{\text{HI}} = \int \sigma_{\text{LC}}(\nu) n_{\nu} d\nu$ is the HI photoionization rate where n_{ν} is the photon number density per frequency. Therefore, the UV background intensity is required to estimate x_{HI} even if we know the clumping factor from the model of the cosmological structure formation. However, it is generally difficult to know the intensity. For this reason, we treat x_{HI} as a free parameter in the following discussions.

The line cross section $\sigma_i(\nu)$ has a very sharp peak at the line center frequency. The width is well characterized by the Doppler width, $\Delta\nu_{\text{D}}$. That is, $\sigma_i(\nu) \simeq \sigma_i$ for $|\nu - \nu_i| \leq \Delta\nu_{\text{D}}$, and $\sigma_i(\nu) \simeq 0$ for $|\nu - \nu_i| > \Delta\nu_{\text{D}}$, where σ_i and ν_i are the cross section and the frequency of the i -th line center, respectively. Since $\nu = \nu_0(1+z)$, we integrate the rhs of equation (4) over a narrow redshift width of $\Delta(1+z) = 2(\Delta\nu_{\text{D}}/\nu_i)(1+z_i)$ around $1+z_i = \nu_i/\nu_0$. Therefore, we obtain

$$\tau_{\nu_0}^i(z_S) \simeq 2 \left[\frac{\sqrt{\pi} e^2 f_i}{m_e c \nu_i} \right] \left[\frac{c n_{\text{HI}}(z_i)}{H(z_i)} \right], \quad (6)$$

where we have substituted $\sigma_i = \sqrt{\pi} e^2 f_i / m_e c \Delta\nu_{\text{D}}$, in which e is the electric charge, f_i is the absorption oscillator strength of the i -th line, and m_e is the electron mass. The values of f_i and ν_i are taken from Wiese, Smith, & Glennon (1966). This time also we are restricted by $z_i \leq z_S$. Thus, the above equation is valid only when $\nu_0 \geq \nu_i/(1+z_S)$, otherwise $\tau_{\nu_0}^i(z_S) = 0$.

For the Ly α line, the opacity becomes

$$\tau^{\text{Ly}\alpha} \simeq 2.6 \times 10^6 x_{\text{HI}}(z) \left(\frac{1+z}{20} \right)^{3/2}, \quad (7)$$

where we approximate $H(z) \approx H_0 \Omega_M^{1/2} (1+z)^{3/2}$ and adopt $n_{\text{HI}}(z) = x_{\text{HI}}(z) n_{\text{H},0} (1+z)^3$. This is the Gunn-Peterson optical depth (Gunn & Peterson 1965; Peebles 1993). From this equation, we realize that if $x_{\text{HI}} \gtrsim 10^{-6}$, the IGM is opaque for the photon bluer than the source Ly α line. Conversely, we can estimate x_{HI} if $\tau^{\text{Ly}\alpha}$ is determined observationally (e.g., Becker et al. 2001; White et al. 2003).

3. NEAR INFRARED SPECTRA

Let us discuss the observed spectra of the GRB afterglows in the NIR bands. To do so, an afterglow spectral model is required. We adopt a simple afterglow model; the synchrotron radiation from the relativistic shock (Sari, Piran, & Narayan 1998). More specifically, we adopt equations (1)–(5) in Ciardi & Loeb (2000) who take into account the effect of the cosmological redshift. The adopted parameters are the magnetic energy fraction of $\epsilon_B = 0.1$, the electron energy fraction of $\epsilon_e = 0.2$, the spherical shock energy of $E = 10^{52} \text{ erg}$, the ambient gas number density of $n = 10 \text{ cm}^{-3}$, and the power-law index of the electron energy distribution $p = 2.5$.

First we consider the observed afterglow spectra in the hypothetical perfectly neutral universe for comparison. In Figure 1, we show the expected afterglow spectra in the neutral universe observed 1 hour after the burst in the observer's frame. Due to the Ly α line absorption, the continuum bluer than the Ly α line in the source frame (the observed wavelength $0.1216[1+z_S] \mu\text{m}$) is completely damped. Thus, we can find the Ly α break clearly. From

³ This assumption is fairly justified even at very high- z universe because the recombination time-scale is much less than the Hubble time-scale.

the observed wavelength of the Ly α break, we can determine the redshift of the GRBs. If we observe the afterglow through a filter, the radiation from the source with the redshift higher than the characteristic redshift of the filter cannot be detected because of the Ly α break. For example, the effect starts from $z_S \simeq 8$ for the J -band and the source with $z_S \gtrsim 11$ cannot be seen through the filter, i.e. J *drop-out*. These characteristic redshifts are summarized in Table 1. However, we have a chance to see the source beyond the drop-out redshift if the universe is highly ionized as we will show later.

Next we examine what is observed if the very high- z universe is ionized completely as proposed by Cen (2003a,b). Let us set the neutral fraction, x_{HI} , of the universe in the redshift range $15 \leq z < 20$ to be very small and $x_{\text{HI}} \sim 1$ for $z < 15$ and $z \geq 20$. That is, we assume that the Pop III stars ionized the universe at $z = 20$ and the sudden change of the IMF due to the transition from the Pop III to II was occurred at $z = 15$. The neutral fraction is determined by the background UV intensity produced by the Pop III stars. However, the intensity is quite uncertain, so that we choose two cases as $x_{\text{HI}} = 10^{-6}$ and 10^{-7} for instance (see also Fig.5 in section 5). We will present a way to constrain x_{HI} from the observations later.

In Figure 2, we show the expected spectra of the GRB afterglows. The solid, short-dashed, long-dashed, dot-dashed, and dotted curves are the expected afterglow spectra of the GRB at $z_S = 22, 20, 18, 15$, and 13 , respectively. The observing time is assumed to be 1 hour after the prompt emission in the observer's frame. We find the clear Ly α breaks in the spectra. Since $x_{\text{HI}} = 10^{-6}$ (or 10^{-7}) at $15 \leq z < 20$ is assumed in the panel (a) (or (b)), the IGM opacity is an order of unity (or 0.1) in the redshift range (see eq.[7]). Thus, the continuum bluer than the Ly α break of the GRBs with $z_S > 15$ still remains of the order of $10 \mu\text{Jy}$ (or $100 \mu\text{Jy}$) in $\sim 2\text{--}2.5 \mu\text{m}$, i.e., in K -band (see the thin solid curve indicated as K ; we adopt the filter system of Bessell & Brett 1988). The spectral break at $1.94(=0.1216[1+15]) \mu\text{m}$ is due to the neutral hydrogen below $z = 15$. Thus, the continuum less than the break wavelength in the observer's frame from the $z_S \geq 15$ source is completely extinguished. The spectra of the source with $z_S < 15$ are the same as those shown in Figure 1. For $z_S = 22$ case, the spectrum shows the second break at $2.36(=0.1026[1+22]) \mu\text{m}$. This is the Ly β break due to the neutral hydrogen near the GRB. Here we have assumed $x_{\text{HI}} \sim 1$ for $z \geq 20$.

The structure corresponding to the reionization history appears in the spectra of the GRB afterglows as shown in Figure 2 (see also Haiman & Loeb 1999). If we could detect the continuum rising at $2.55(=0.1216[1+20]) \mu\text{m}$ in the spectrum of the GRB with $z_S = 22$, we would find the starting epoch of the first reionization as $z = 20$. On the other hand, the end of the first reionization, in other words, the transition epoch from the Pop III to II is realized from the spectral break at $1.94(=0.1216[1+15]) \mu\text{m}$.

The suitable band to determine the ionization history depends on the redshift of the reionization epoch. From Figure 1 (see also Table 1), we find that the I , J , H , and K -band spectroscopies are suitable for the reionization epoch at $z \simeq 5\text{--}7, 8\text{--}11, 11\text{--}14$, and $15\text{--}20$, respectively. In

any case, observations to detect the spectral signatures in the NIR afterglow spectra of the GRBs are strongly encouraged. If x_{HI} were smaller than 10^{-6} , we would clearly see the difference from Fig. 1 and could confirm the double reionization.

In the above discussion, we assumed $x_{\text{HI}} = 10^{-6}$ and 10^{-7} . Let us argue what will happen for different values of x_{HI} . If $x_{\text{HI}} \gtrsim 10^{-6}$, the remaining flux decreases exponentially because the IGM opacity becomes much larger than unity; for example, the flux is about 1 nJy for $x_{\text{HI}} = 6 \times 10^{-6}$, and about 1 pJy for $x_{\text{HI}} = 10^{-5}$. It is quite difficult to detect such a low-level flux. Even if $x_{\text{HI}} \gtrsim 10^{-6}$, however, we have a chance to obtain the information of the IGM ionization state because the absorption is made by the intervening neutral *clouds*. That is, we may detect the continuum escaping from a number of line absorptions by using a high dispersion spectrograph. This is a very challenging observation.

4. NEAR INFRARED COLORS

The photometric observations are available easier than the spectroscopy. We examine the expected apparent NIR colors of the GRB afterglows. Although we can discuss the apparent magnitude of the afterglows in one photometric filter, their dispersion is very large because the luminosity of the afterglows depends on many uncertain parameters such as the jet opening angle, the ambient matter density, the magnetic energy fraction and the relativistic electron energy fraction. On the other hand, the dispersion of the apparent colors can be quite small because the color does not depend on the absolute luminosity but only the spectral shape which does not change significantly in the observed NIR bands.

The apparent magnitude⁴ in a filter band denoted as i is defined by

$$m_i = -2.5 \log F_i / F_{i,0}, \quad (8)$$

where $F_{i,0}$ is the zero point flux density of the filter and F_i is the mean flux density through the filter which is

$$F_i = \frac{\int T_{i,\nu} f_\nu e^{-\tau_\nu} d\nu}{\int T_{i,\nu} d\nu}, \quad (9)$$

where $T_{i,\nu}$ is the transmission efficiency of the filter and $f_\nu e^{-\tau_\nu}$ is the flux density entering the filter. If there is no intervening absorber between the source and the telescope, $\tau_\nu = 0$.

The observed color between two filter bands, i and j (the filter i is bluer than the filter j), is given by

$$m_i - m_j = (m_i - m_j)^{\text{int}} + (\Delta m_i - \Delta m_j), \quad (10)$$

where $(m_i - m_j)^{\text{int}}$ is the intrinsic color of the source, and Δm_i and Δm_j are the absorption amounts in the filters i and j , respectively. When we consider the NIR filter bands and high- z GRBs (for example $z = 15$), the intrinsic afterglow spectrum is predicted to be proportional to $\nu^{-1/2}$ from ~ 1 minute to several hours after the burst occurrence and proportional to $\nu^{-p/2}$ for later time in the standard afterglow model (Sari, Piran, & Narayan 1998; Ciardi & Loeb 2000). Other parameters adopted are described in the beginning of the section 3. In Table 2, we tabulate the intrinsic colors of the sources for the two cases of the spectral shape.

⁴ All magnitudes in this paper are the Vega system.

The absorption amount in the filter i is

$$\Delta m_i \equiv m_i - m_i^{\text{int}} = -2.5 \log \frac{\int T_{i,\nu} f_\nu e^{-\tau_\nu} d\nu}{\int T_{i,\nu} f_\nu d\nu}, \quad (11)$$

where $m_i^{\text{int}} = m_i(\tau_\nu = 0)$ is the intrinsic (no absorption) apparent magnitude. In a certain band width $\Delta\nu$, the difference in the optical depth $\Delta\tau$ is estimated as $|\Delta\tau/\tau| = 3/2(1+z)^{-1}|\Delta(1+z)| \sim (1+z)^{-1}|\Delta\nu/\nu|$ from equation (7). Since $\Delta\nu$ of the filter transmission is smaller than the effective frequency of the filter, i.e. $\Delta\nu/\nu < 1$, and also $z \gtrsim 5$, $\Delta\tau/\tau \ll 1$, that is, the term $e^{-\tau_\nu}$ in the integral of the numerator in equation (11) can be regarded as almost constant. Hence, we obtain approximately $\Delta m_i \approx 1.086\tau_{\text{eff}}$, where τ_{eff} is the effective IGM opacity in the filter i .

Now we can estimate the observed color by equation (10) if Δm_i is known. To know Δm_i is equivalent to know the IGM effective opacity τ_{eff} . This opacity is one between the redshift at which the Ly α break comes into the filter band width ($z_{\text{Ly}\alpha,\text{in}}^i$, see Table 1) and the source redshift (z_S) because the neutral hydrogen in $z < z_{\text{Ly}\alpha,\text{in}}^i$ cannot absorb the photons passing through the filter i . We note that the neutral hydrogen lying beyond the redshift at which the Ly α break goes out of the filter band width ($z_{\text{Ly}\alpha,\text{out}}^i$, see Table 1) absorb the photons through the filter i because of the higher-order Lyman series lines like Ly β , Ly γ , etc., and the photoionization process. As a result, τ_{eff} is determined by the neutral fraction x_{HI} in the redshift range $z_{\text{Ly}\alpha,\text{in}}^i \leq z \leq z_S$. Since x_{HI} at high- z is uncertain, we assume that x_{HI} is constant in the above range for simplicity. The real x_{HI} might vary significantly in the redshift range, so that the assumed x_{HI} should be regarded as an effective mean value including such a variation (hereafter $x_{\text{HI}}^{\text{eff}}$).

In Figures 3a–3d, we show Δm_i for the I , J , H , and K -bands as a function of the source redshift. The continuum in the observer's L -band is not absorbed by the IGM neutral hydrogen at all when the source redshift is less than about 25. Although we assumed that the spectral shape is proportional to $\nu^{-1/2}$ in the panels, the results are much robust for the change of the spectral shape as noted above. The solid curves in these panels are loci of Δm_i for a given $x_{\text{HI}}^{\text{eff}}$ as a function of the source redshift z_S . For example, since $z_{\text{Ly}\alpha,\text{in}}^I = 5$ for I -band, the IGM absorption in I -band is about 5 mag for the source at $z_S = 7$ if the effective neutral fraction $x_{\text{HI}}^{\text{eff}}$ in the redshift range $5 \leq z \leq 7$ is 10^{-5} .

Two dotted vertical lines in each panel of Figure 3 indicate the redshifts when the Ly α break enters and goes out of the each band width ($z_{\text{Ly}\alpha,\text{in}}^i$ and $z_{\text{Ly}\alpha,\text{out}}^i$, respectively). As seen in Figure 1, if the IGM is significantly neutral, the source with $z_S > z_{\text{Ly}\alpha,\text{out}}^i$ cannot be detected through the filter i (i.e. *drop-out*). However, we can detect such a source if the universe is highly ionized. This is because the continuum below the Ly α break remains as shown in Figure 2.

Suppose we observe a source with $z_S > z_{\text{Ly}\alpha,\text{out}}^i$ through the i and j filters and assume that the radiation through j filter is not affected by any intervening absorption (i.e. $\Delta m_j = 0$). From equation (10), the expected magnitude through the i filter is

$$m_i = m_j + (m_i - m_j)^{\text{int}} + \Delta m_i. \quad (12)$$

For example, we consider the case of $i = I$, $j = L$, and $z_S = 7$. We find that the apparent L magnitude of the afterglow of the GRB at $z_S = 7$ for 1 hour after the prompt burst is about 14 mag from Figure 4. Thus, the apparent I magnitude is expected to be 22 mag because the intrinsic $I - L = 3.1$ mag for 1 hour (i.e. the case $\propto \nu^{-1/2}$ in Table 2) and $\Delta I \sim 5$ mag if $x_{\text{HI}}^{\text{eff}} = 10^{-5}$ in the redshift range $5 \leq z \leq 7$. We can reach 5- σ detection of the source with $I = 22$ mag by only three minutes exposure with a 8-m class telescope. Interestingly the assumed $x_{\text{HI}}^{\text{eff}}$ is similar to the value reported by White et al. (2003) from the Gunn–Peterson trough in the spectra of $z > 6$ quasars.

Similar argument can be done for other bands. Therefore, in general, the detection of the source with $z_S > z_{\text{Ly}\alpha,\text{out}}^i$ through the filter i is the very good evidence that the universe in the redshift range $z_{\text{Ly}\alpha,\text{in}}^i \lesssim z \lesssim z_S$ is highly ionized, i.e. $x_{\text{HI}}^{\text{eff}} \ll 1$ in that redshift range. Conversely, the detection enables us to estimate τ_{eff} and $x_{\text{HI}}^{\text{eff}}$. Finally, we note here that Figure 3 is also useful for any other sources because Δm_i is almost independent of the source spectrum.

5. DISCUSSIONS

5.1. Was the universe reionized twice?

Here we discuss how we can confirm or refute Cen's scenario: the universe was reionized twice. In the scenario, the first complete ionization at $z \sim 20$ is followed by the partially ionized epoch at $z \sim 10$. Therefore, we should check whether the neutral fraction at $z \sim 20$ is very low or not and whether the fraction at $z \sim 10$ is almost unity or not. To do so, the best observation is the spectroscopy in the NIR bands. As shown in Fig. 2 of section 3, the reionization history is imprinted in the observed continuum. However, the sensitivity of the spectroscopy is in general much less than that of the photometric observations. Hence we discuss the way using the NIR photometries.

In the previous section, we have shown that the detection of the GRB afterglows through a filter i beyond the Ly α drop-out redshift ($z_{\text{Ly}\alpha,\text{out}}^i$) proves the ionization of the universe around $z_{\text{Ly}\alpha,\text{out}}^i$. From the characteristic redshifts for the NIR filters summarized in Table 1, the I , J , H , and K filters are the suitable to check the ionization state at $z \sim 5\text{--}8$, $8\text{--}11$, $11\text{--}15$, and $15\text{--}20$, respectively. Thus, the null detection of the GRB afterglows of $z_S \sim 11$ in J -band indicates an high neutral fraction in $8 \lesssim z \lesssim 11$. On the other hand, we detect the GRB afterglows of $z_S \sim 20$ in K -band if the IGM in $15 \lesssim z \lesssim 20$ is ionized. I and H -band surveys are also very important to assess the reionization history of the universe. We can constrain the latest reionization epoch by observing the GRB afterglows at $z \gtrsim 6$ through I -band. In summary, we can examine the reionization history by checking whether the high- z GRB afterglows drop out of the NIR filters or not.

In the rest of this subsection, we discuss what is the difference between Cen's scenario and others. To demonstrate the main feature, we assume two schematic reionization histories; (1) once gradual reionization and (2) twice sudden reionizations, which are shown in Figure 5 as the solid and dashed curves, respectively. These histories are based on two observational constraints; (1) the

neutral fraction of hydrogen $x_{\text{HI}} \sim 10^{-5}$ at $z \sim 6$ from the Gunn-Peterson trough found in the $z > 6$ quasars spectra (Becker et al. 2001; White et al. 2003), and (2) the beginning of the reionization is $z \sim 20$ from the large opacity of the electron scattering suggested by *WMAP* (Kogut et al. 2003). For the twice reionizations, we also consider different values of x_{HI} in the first reionization epoch.

In Figure 6, we show the expected NIR colors as a function of the source redshift for the afterglow spectrum $f_\nu \propto \nu^{-1/2}$ case (the observing time less than several hours, see Table 2). We find differences between the once and twice reionizations in the $I - J$ (panel [a]) and $K - L$ (panel [d]) colors. In panel (a), the GRB afterglows up to $z_S \sim 8$ can be seen in both of the I and J bands for the once reionization case, whereas the $I - J$ color of $z_S > 7.1$ afterglows diverges in the twice reionization case, i.e. the sources drop out of the I -band. This reflects the difference of the increasing rate of the neutral fraction around $z \sim 6$ in two reionization histories. The drop-out redshift in the twice reionization case is determined by $\lambda_\beta(1 + z_{S,\text{drop}}) = \lambda_\alpha(1 + z_{\text{reion}})$, where λ_α and λ_β are the rest-frame wavelength of the Ly α and Ly β lines, and z_{reion} is the sudden reionization redshift (Haiman & Loeb 1999). In our case, $z_{\text{reion}} = 6$. It is worth to noting that the GRB afterglows beyond the drop-out redshift of the I -band ($z_{\text{Ly}\alpha,\text{out}}^I = 6.6$) can be seen through the filter in both of reionization histories.

In panel (d) of Figure 6, we find a significant difference between the two reionization scenarios. While the afterglows beyond the drop-out redshift of the K -band really drop out of the filter for the once reionization, we can see such afterglows in the twice reionized universe. On the other hand, the afterglows with $z_S > 23$ drop out of the K -band even in the twice reionization case because the Ly β break goes out of the filter transmission width, i.e. $\lambda_\beta(1 + z_{S,\text{drop}}) = \lambda_{\text{max}}^K [= \lambda_\alpha(1 + z_{\text{Ly}\alpha,\text{out}}^K)]$, where λ_{max}^K is the maximum wavelength of the K -band filter. We note here that $z_{\text{reion}} (= 20) > z_{\text{Ly}\alpha,\text{out}}^K$ in this time, whereas $z_{\text{reion}} (= 6) < z_{\text{Ly}\alpha,\text{out}}^I$ in the above case.

Any difference between the once and twice reionizations cannot be found in the $J - H$ (panel [b]) and the $H - K$ (panel [c]) colors because the neutral fractions in both cases are high enough ($\gtrsim 10^{-4}$) to extinguish the continuum bluer than the Ly α break completely. That is, the GRB afterglows beyond the drop-out redshift cannot be seen in the J and H -bands for both of reionization histories.

Let us summarize how to confirm or refute Cen's scenario: We can conclude that the universe was reionized twice if (1) the GRB afterglows with $z_S > z_{\text{Ly}\alpha,\text{out}}^K$ is detected in the K -band and (2) the afterglows with $z_S > z_{\text{Ly}\alpha,\text{out}}^J$ or $z_S > z_{\text{Ly}\alpha,\text{out}}^H$ drop out of the J or H -bands. However, the null detection of the $z_S > z_{\text{Ly}\alpha,\text{out}}^K$ GRB afterglows in the K -band does not reject Cen's scenario at once. The null detection only shows the neutral fraction at $z \sim 20$ larger than $\sim 10^{-5}$. In any case, the deep and prompt K -band photometry of the high- z GRB afterglows is useful to examine the ionization state at $z \sim 20$ very much.

5.2. Comment on Lyman break technique

In the above discussions, we assumed that the GRB redshifts are known from other methods. Although the spectroscopy of the optical afterglow or the host galaxies is used to determine the redshift of the low- z GRBs, it may be difficult for the high- z GRBs. The Fe line in the X-ray afterglow (Mészáros & Rees 2003) or some empirical ways using the γ -ray data alone (Norris et al. 2000; Ioka & Nakamura 2001; Atteia 2003) can be useful for the high- z GRBs. In addition, the search for the Ly α break is considered to be useful. Indeed, the spectroscopic detection of the sharp Ly α cut-off (see Figs.2 and 3) is an accurate method to determine the redshift. However, the color selection technique which is often used to find the $z \gtrsim 3$ galaxies (Madau 1995; Steidel et al. 1996) may not be good for the high- z GRBs. This is because the GRB afterglows beyond the drop-out redshift of the considered filter can be detectable if the universe is ionized enough.

For example, if we use $I - J \geq 5$ mag as a criterion to select the high- z GRBs, the selected objects have $z \gtrsim 6.5$ indeed (see Fig.3a and Table 2). However, a number of real $z \gtrsim 6.5$ objects escape the criterion if the neutral fraction is less than $\sim 10^{-5}$. Therefore, we cannot use a simple color selection technique for the high- z GRBs. Spectroscopic observations to detect the Ly α break feature and Fe line, or some empirical methods are required.

5.3. Advantage and disadvantage of NIR colors method

The largest advantage of the NIR color method is its easier availability and higher sensitivity than other methods. The limiting magnitude with a high signal-to-noise ratio of the broad-band NIR photometry reaches much deeper than 20 mag by only a few minute exposure with a 8-m class ground based telescope. For example, the IRCS (Infrared Camera and Spectrograph) equipped with the Subaru telescope (Japanese 8-m class telescope⁵) can reach the 2σ upper limit of 22 mag by only five minutes exposure in K -band. This magnitude corresponds to $\Delta K \simeq 5$ mag based on the expected L magnitude of $\simeq 16$ mag for the $z \simeq 20$ GRB afterglows at 1 hour after the burst (Fig.4) and $K - L = 1.1$ (Table 2), and also corresponds to the neutral fraction of 3×10^{-6} . Thus, we can put this value as a lower limit of the neutral fraction at $z \sim 20$ for null detection. A more strict lower limit can be obtained if we observe the afterglows as early as possible. In addition, the apparent magnitude becomes ~ 5 –6 mag brighter than that shown in Figure 4 if we observe the emission from the reverse shock (Gou et al. 2003). A very early observation is highly desired.

From the detected magnitude or the limiting magnitude for the null detection, the neutral fraction or its lower limit in the corresponding redshift range can be estimated. However, the uncertainty of the obtained neutral fraction may be large if we have only one photometric data. This is because the apparent dispersion of the afterglow luminosities is large. Even in that case, the uncertainty can be controlled in a low level if we use more than two photometric data, i.e. colors, which are independent of the absolute luminosity. This point is one of the important advantages of the NIR color method. Therefore, the NIR multi-colors follow-ups of the GRB afterglows are strongly encouraged.

⁵ <http://subarutelescope.org/>

Miralda-Escudé (1998) and Barkana & Loeb (2003) show that the detailed spectroscopy of the red damping wing of the Ly α break provides us with the neutral hydrogen column density to the source. However, the spectral resolution required is $\lambda/\Delta\lambda \gtrsim 1000$. The limiting magnitude for such observations becomes much shallower than that of the photometry. Moreover, a huge number of Earth's atmospheric OH lines are contaminated in the spectra of the NIR bands obtained with the ground-based telescope. Only JWST (James Webb Space Telescope)⁶ will have such a high spectral resolution among the future space telescopes having the NIR spectrograph. Thus, we must await its launch to discuss the shape of the damping wing.

The disadvantage of the NIR color method is the coarse redshift resolution. As discussed in section 4, the neutral fraction obtained by the color method is an averaged one in the redshift range of $z_{\text{Ly}\alpha,\text{in}} \leq z \leq z_{\text{S}}$. Thus, we cannot determine the so-called reionization redshift. Only the redshift range in which the reionization occurred is obtained. However, even such a rough redshift resolution is enough to discuss whether the reionization is once, twice,

or more.

To know the detailed history of the reionization, the spectroscopy is needed. For this purpose, the Japanese astronomical satellite ASTRO-F⁷ can be useful. The satellite will have the spectroscopic sensitivity of $\sim 30 \mu\text{Jy}$ around $\sim 2 \mu\text{m}$, which can detect the GRB afterglows of $z_{\text{S}} \sim 20$ if $x_{\text{HI}} \sim 10^{-6}$ (see Fig.2a). SIRTF (Spece InfraRed Telescope Facility)⁸ may not be useful because it has the sensitivity only in the wavelength longer than $5 \mu\text{m}$. In future, JWST is much promising. Finally, we note that the narrow-band photometry may be useful because its narrow transmission width provides us with a moderate resolution of redshift keeping a higher sensitivity than that of spectroscopy.

This work is supported in part by the Grant-in-Aid for Scientific Research of the Japanese Ministry of Education, Culture, Sports, Science and Technology, No.14047212 (TN), and No.14204024 (TN). AKI and RY thank the Research Fellowships of the Japan Society for the Promotion of Science for Young Scientists.

REFERENCES

Atteia, J.-L. 2003, A&A, 407, L1
 Barkana, R. & Loeb, A. 2003, ApJ, submitted (astro-ph/0305470)
 Becker, R. H., et al. 2001, AJ, 122, 2850
 Bessell, M. S. 1990, PASP, 102, 1181
 Bessell, M. S., & Brett, J. M. 1988, PASP, 100, 1134
 Cen, R. 2003a, ApJ, 591, 12
 Cen, R. 2003b, ApJ, 591, L5
 Chiu, W. A., Fan, X., & Ostricker, J. P. 2003, ApJ, submitted (astro-ph/0304234)
 Ciardi, B. & Loeb, A., 2000, ApJ, 540, 687
 Ciardi, B., Ferrara, A., & White, S. D. M. 2003, MNRAS, submitted (astro-ph/0302451)
 Galama, T.J., et al. 1998, Nature, 395, 670
 Gou, L. J., Mészáros, P., Abel, T., & Zhang, B. 2003, ApJ, submitted (astro-ph/0307489)
 Gunn, J. E., & Peterson, B. A. 1965, ApJ, 142, 1633
 Haiman, Z., & Loeb, A. 1999, ApJ, 519, 479
 Haiman, Z., & Holder, G. P. 2003, ApJ, submitted (astro-ph/0302403)
 Hjorth, J. et al., 2003, Nature, 423, 847
 Ioka, K., & Nakamura, T. 2001, ApJ, 554, L163
 Kogut, A., et al. 2003, ApJ, in press (astro-ph/0302213)
 Lamb, D.Q., Reichart, D.E. 2000, ApJ, 536, 1
 Loeb, A., & Barkana, R. 2001, ARA&A, 39, 19
 Madau, P. 1995, ApJ, 441, 18
 Mészáros, P. & Rees, M.J. 2003, ApJ, 591, L91
 Miralda-Escudé, J. 1998, ApJ, 501, 15
 Nakamoto, T., Umemura, M., & Susa, H. 2001, MNRAS, 321, 593
 Norris, J.P., Marani, G.F., & Bonnell, J.T. 2000, ApJ, 534, 248
 Onken, C. A., & Miralda-Escudé, J. 2003, ApJ, submitted (astro-ph/0307184)
 Osterbrock, D. E. 1989, *Astrophysics of Gaseous Nebulae and Active Galactic Nuclei* (Mill Valley: University Science Books)
 Peebles, P. J. E. 1993, *Principles of physical cosmology*, Princeton University Press, New Jersey
 Price, P.A. et al., 2003, Nature, 423, 844
 Sari, R., Piran, T., & Narayan, R. 1998, ApJ, 497, L17
 Sokasian, A., Yoshida, N., Abel, T., Hernquist, L., & Springel, V. 2003, astro-ph/0307451
 Spergel, D., et al. 2003, ApJ, in press (astro-ph/0302209)
 Steidel, C. C., Giavalisco, M., Pettini, M., Dickinson, M., & Adelberger, K. L. 1996, ApJ, 462, L17
 Uemura, M. et al. 2003, Nature, 423, 843
 White, R. L., Becker, R. H., Fan, X., & Strauss, M. A. 2003, AJ, 126, 1
 Wiese, W. L., Smith, M. W., & Glennon, B. M. 1966, *Atomic Transition Probabilities*, Vol. 1 (NSRDS-NBS 4; Washington: GPO)

Wyithe, J. S. B., & Loeb, A. 2003a, ApJ, 586, 693
 Wyithe, J. S. B., & Loeb, A. 2003b, ApJ, 588, L69

⁶ <http://ngst.gsfc.nasa.gov/>

⁷ <http://koala.ir.isas.ac.jp/ASTRO-F/index-e.html>

⁸ <http://sirtf.caltech.edu/>

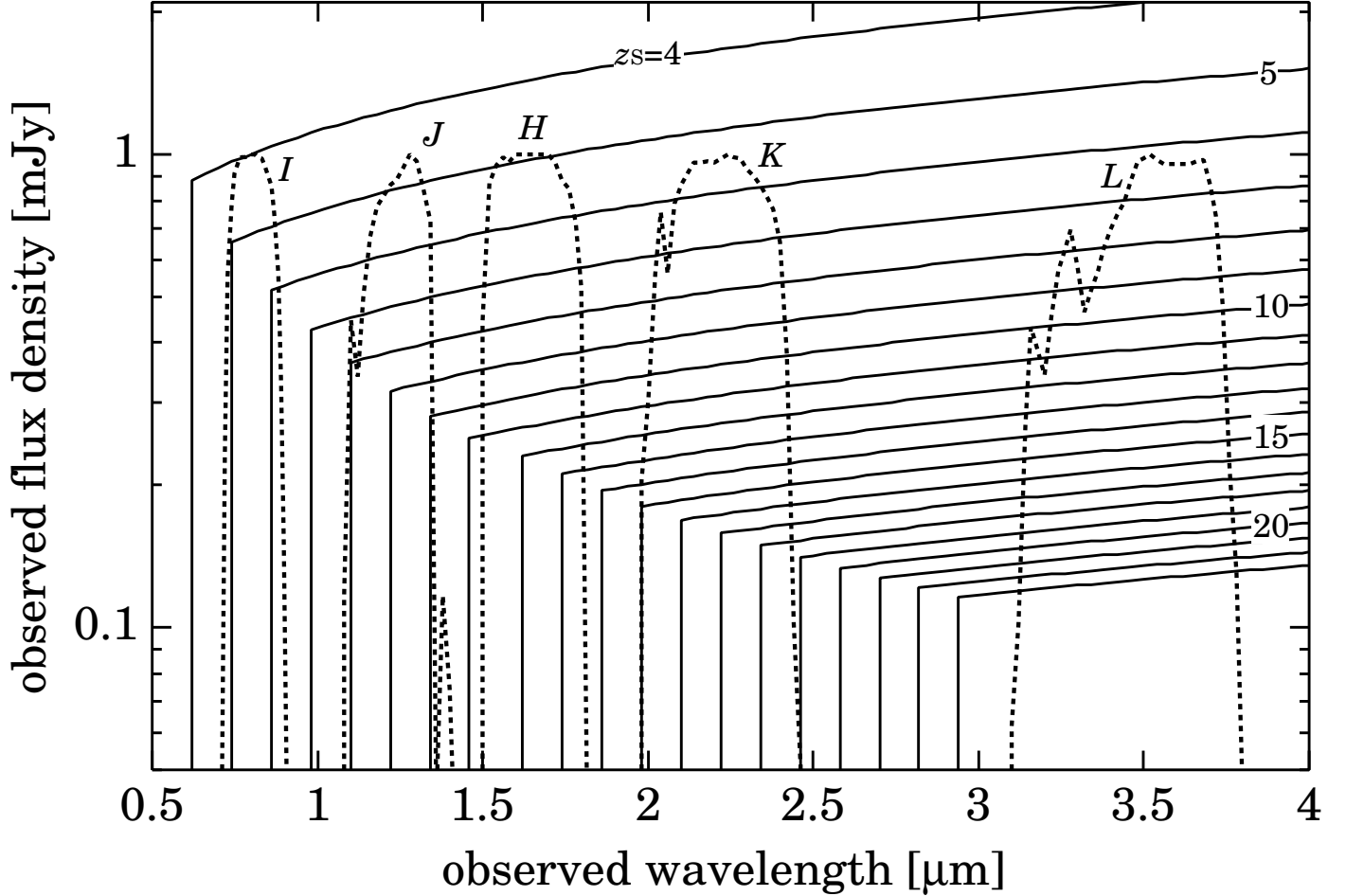


FIG. 1.— Afterglow spectra in the hypothetical neutral universe. The solid curves are the afterglow spectra of the gamma-ray bursts at the redshift $z_S = 4-23$ as indicated in the panel. The observing time is set to be 1 hour after the burst for all curves. The dotted curves are the filter transmissions of I , J , H , K , and L bands (Bessell & Brett 1988; Bessell 1990). These transmission curves are scale free.

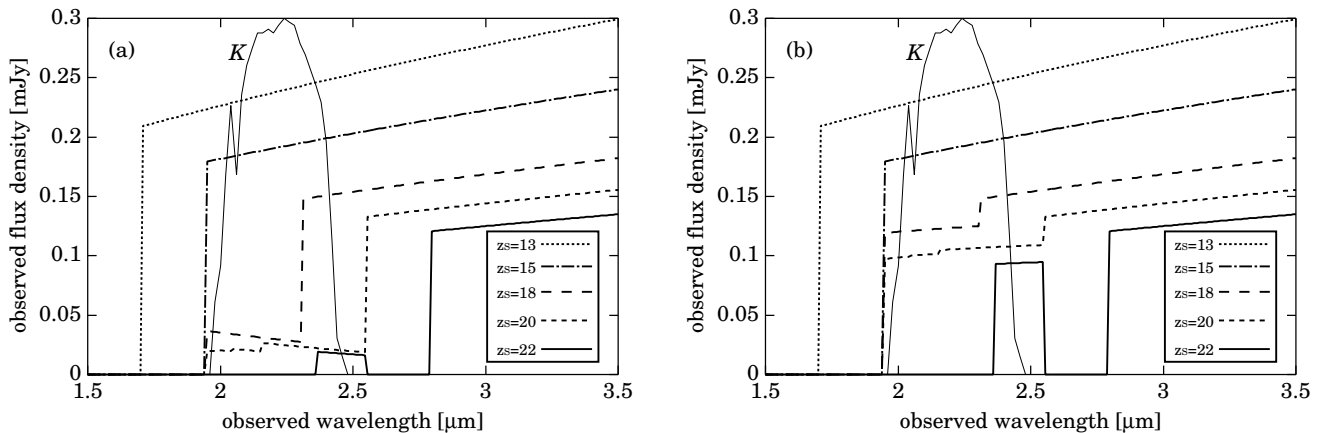


FIG. 2.— Expected near-infrared afterglow spectra of very high redshift gamma-ray bursts. The solid, short-dashed, long-dashed, dot-dashed, and dotted curves are the cases of the source redshift $z_S = 22, 20, 18, 15$, and 13 respectively. The observing time is set to be 1 hour after the burst for all curves. The neutral fraction in $15 \leq z < 20$ is assumed to be 10^{-6} and 10^{-7} for the panels (a) and (b), respectively. The thin solid curve is the filter transmission of K -band (Bessell & Brett 1988). This transmission curve is scale free.

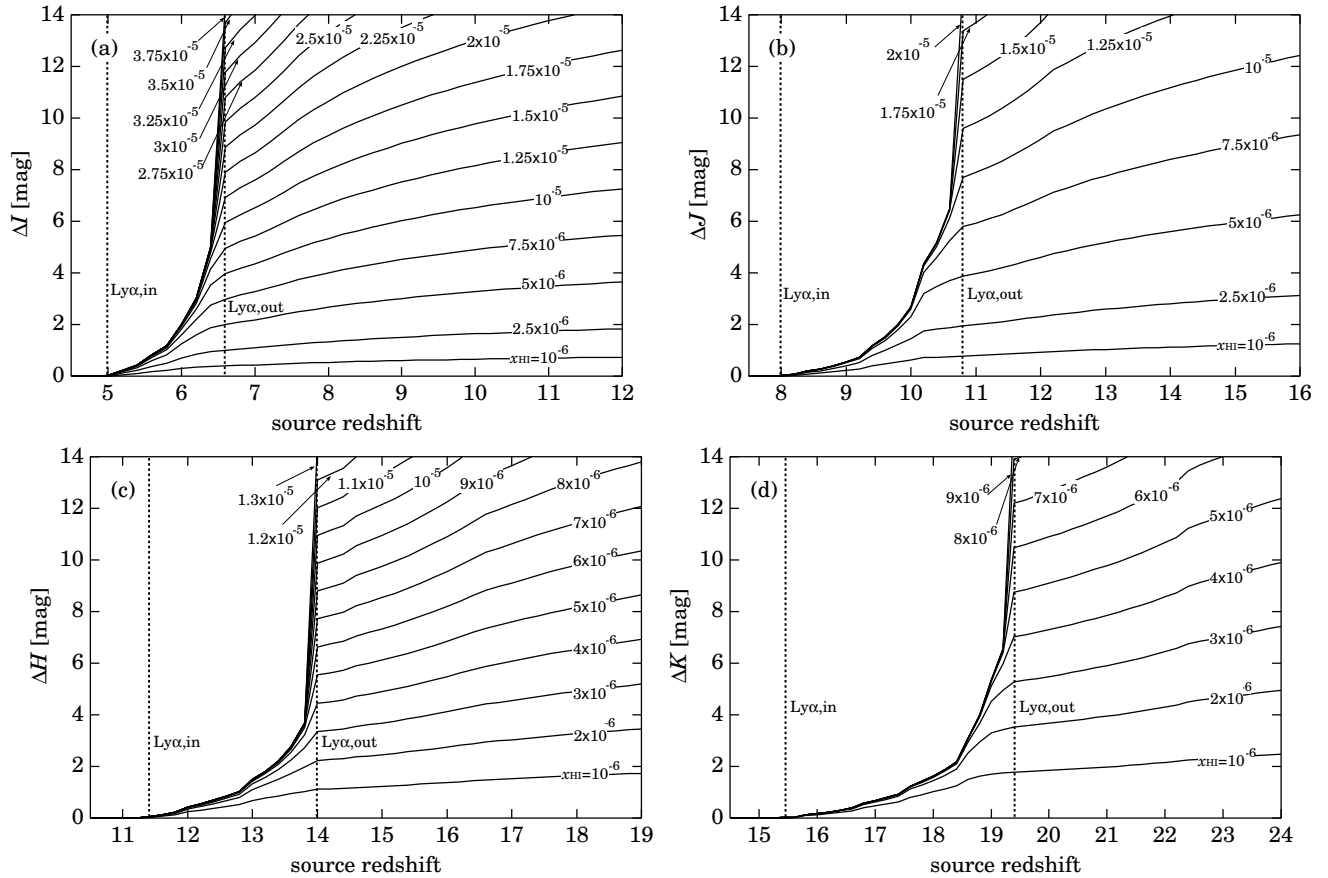


FIG. 3.— The intergalactic absorption in near-infrared bands. The vertical axis in each panel means the absorption amount in each filter (see eq.[11]); (a) I -band, (b) J -band, (c) H -band, and (d) K -band. The solid curves in the panels are loci of the absorption amount as a function of the redshift of the source z_S . The neutral hydrogen fraction, x_{HI} , is assumed to be constant between the redshift when the Ly α break enters the filter transmission and z_S . The assumed x_{HI} is indicated on each curve. Two dotted vertical straight lines in each panel indicate the source redshifts at which the Ly α break enters and goes out of the filter.

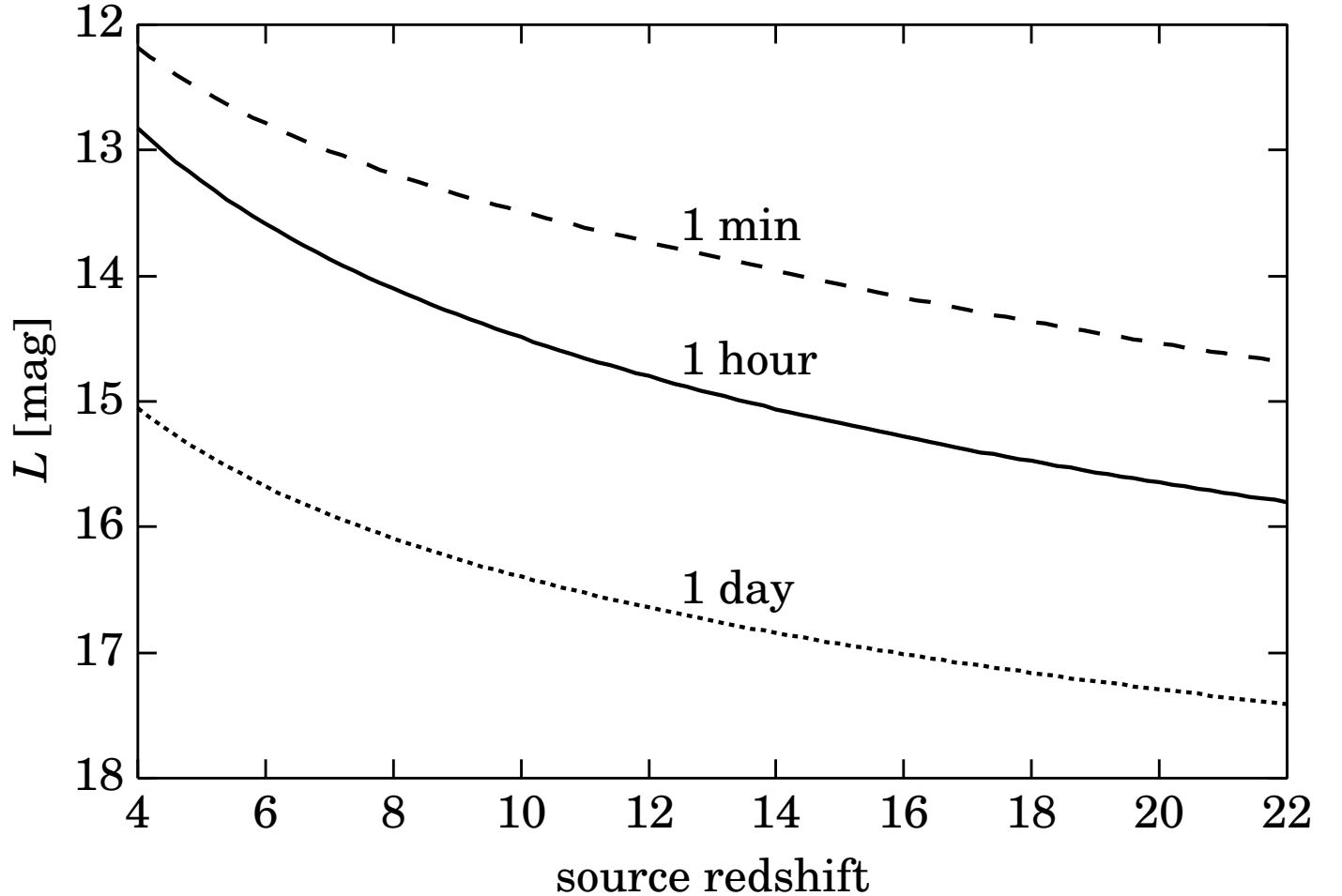


FIG. 4.— The expected apparent magnitude in L -band of the afterglows of the gamma-ray bursts (GRBs) as a function of the source redshift. The dashed, solid, and dotted curves are the cases of 1 minute, 1 hour, and 1 day after the burst occurrence in the observer's frame, respectively. The spectral model of the GRB afterglows by Ciardi & Loeb (2000) is adopted. The assumed parameter set is described in the first paragraph of section 3.

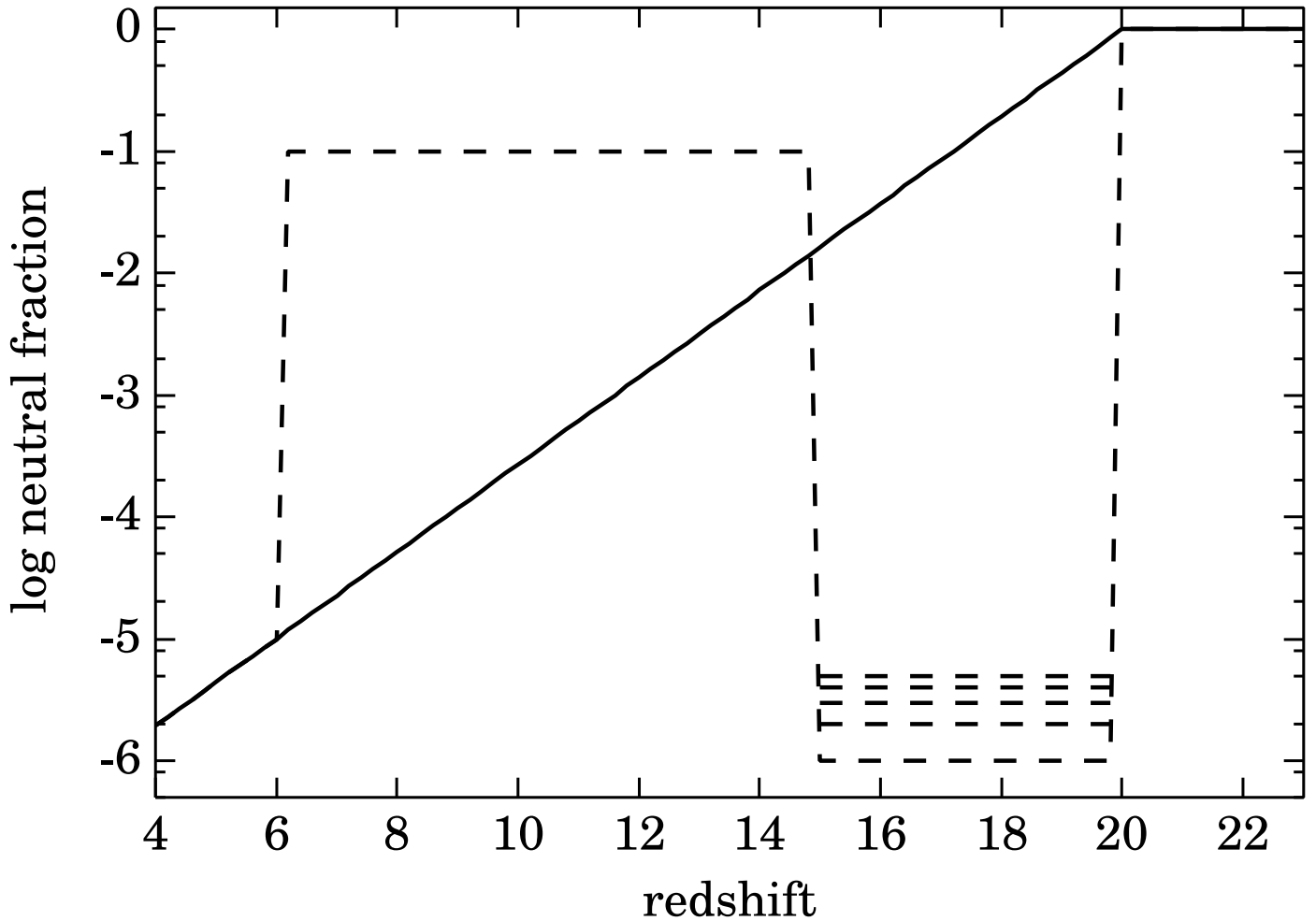


FIG. 5.— Examples of the reionization history. The solid curve is a gradual reionization case. The dashed curve is a twice reionization case as suggested by Cen (2003a).

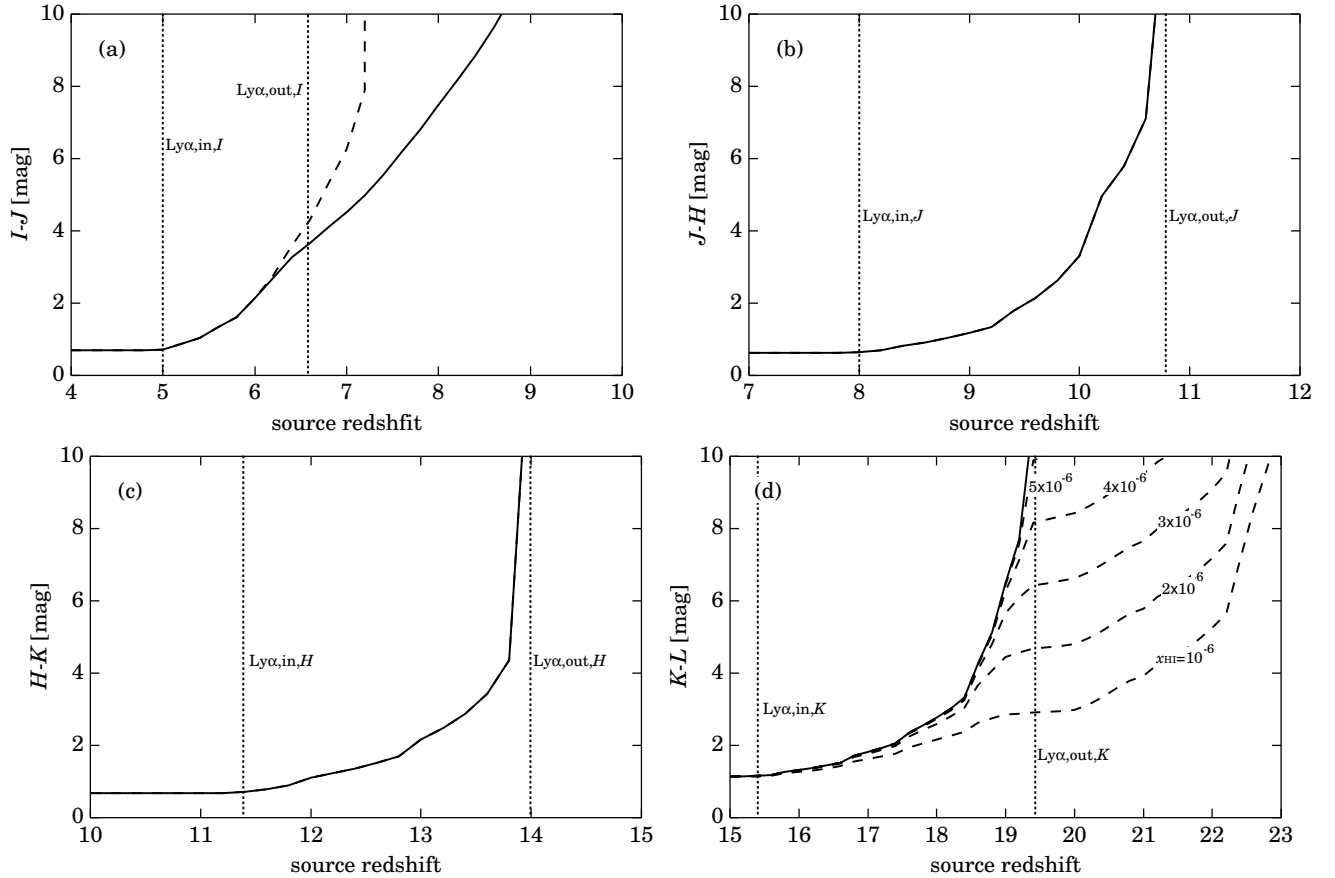


FIG. 6.— Expected near-infrared colors of gamma-ray burst afterglows. (a) $I - J$ colors, (b) $J - H$ colors, (c) $H - K$ colors, and (d) $K - L$ colors. The solid and dashed curves correspond to the cases of the once and twice reionizations depicted in Figure 5, respectively. The solid and dashed curves in panels (b) and (c) are perfectly superposed. In panel (d), some cases of the neutral hydrogen fraction in the first reionization are shown. Two dotted vertical straight lines in each panel indicate the source redshifts at which the Ly α break enters and goes out of the indicated filter.

TABLE 1
CHARACTERISTIC REDSHIFTS OF NIR FILTERS

filter	$z_{\text{Ly}\alpha,\text{in}}$	$z_{\text{Ly}\alpha,\text{out}}$
<i>I</i>	5.0	6.6
<i>J</i>	8.0	10.8
<i>H</i>	11.4	14.0
<i>K</i>	15.4	19.4
<i>L</i>	24.6	30.6

Note. — $z_{\text{Ly}\alpha,\text{in}}$ and $z_{\text{Ly}\alpha,\text{out}}$ are the redshifts at which the Ly α break enters and goes out of the filter transmission, respectively.

TABLE 2
NIR AFTERGLOW INTRINSIC COLORS

color	$\propto \nu^{-1/2}$	$\propto \nu^{-p/2}$ ($p = 2.5$)
<i>I</i> – <i>J</i>	0.70	1.0
<i>I</i> – <i>H</i>	1.3	1.9
<i>I</i> – <i>K</i>	2.0	2.8
<i>I</i> – <i>L</i>	3.1	4.3
<i>J</i> – <i>H</i>	0.62	0.86
<i>J</i> – <i>K</i>	1.3	2.8
<i>J</i> – <i>L</i>	2.4	3.3
<i>H</i> – <i>K</i>	0.67	0.91
<i>H</i> – <i>L</i>	1.8	2.4
<i>K</i> – <i>L</i>	1.1	1.5

Note. — In the observer's frame, the NIR afterglow spectrum of the GRBs at $z \sim 10$ is proportional to $\nu^{-1/2}$ between ~ 1 minute and several hours after the initial burst and proportional to $\nu^{-p/2}$ for later time.